Final Report for AOARD Grant FA48690814052

"Improvement of thermoelectric-properties for Mg-based quaternary compounds with doping via bulk mechanical alloying"

05/02/2010

Name of Principal Investigators: Tatsuhiko Aizawa

- e-mail address : taizawa@sic.shibaura-it.ac.jp
- Institution : Shibaura Institute of Technology
- Mailing Address : 3-9-14 Shibaura, Minato, Tokyo 108-8548 Japan
- Phone : +81-3-6722-2741
- Fax : +81-3-6722-2641

Period of Performance: 03/08/2007 – 02/07/2009

Abstract:

In the magnesium base TE material design, the solid solution formation is favored for reduction of thermal conductivity by lattice scattering effect. Since magnesium and silicon have low relative density, Mg2Si-base TE compounds are expected to improve the specific figure-of-merit. In this project, new material processing route is proposed and developed to make material search for ternary or quartic TE compounds and to make mass-production of Mg_2Si-base TE materials. Effect of Si, Ge and Sn on the thermoelectricity is also discussed to find an optimum way of TE-materials design.

Introduction:

Magnesium has binary, ternary and quartic compounds together with silicon, germanium, tin a nd lead. In particular, ternary compounds like Mg-Si-Ge and Mg-Si-Sn become a starting mat erial system, on the basis of which the alloy design is based to improve the figure-of-merit o r the specific figure-of-merit. Mg-Si-Ge system has complete solid-solubility like Ge-Si system 1); thermoelectric properties are designable with variation of germanium concentration 2). Mg-Si-Sn system is reported to have a significant solid-solubility both in the Sn-deficient and Sn-enriched content regions; phase separation to Mg_2Si + Mg_2Sn is reported to take place in the middle Sn-content region 3). In the most of literature, samples are prepared by the melting and solidification process; the above solid solution formation and phase separation must be reconsidered by the solid-state synthesis.

The melting and solidification method 4-6) suffers from many difficulties in practice: relatively high melting point of Si and Ge, and, their chemical reaction with constituents of crucibles. Since magnesium has high vaporizing pressure and Si and Ge have high melting point, it is difficult or nearly impossible to accurately control the molar ratio among Mg, Si, Ge and Sn. In addition, Mg-Si-Ge system has deliquescene in the germanium rich regions. In the powder metallurgy, mechanical milling and grinding have been utilized for fabrication of sintered samples 7, 8). Hot pressing and spark plasma sintering were also used at relatively high temperature to yield dense samples 8). During milling, pure magnesium and Si/Ge are easy to be adhesive or reacted with the constituents of vials and balls. Since the refined magnesium powders are inflammable, the processed sample is never free from oxidation. These conventional materials processing is difficult to describe thermoelectricity of solid-solution type semi-conductive materials. In addition, their mass-production in the industrial applications is beyond capacity for these methods.

The bulk mechanical alloying (BMA) is expected to fabricate magnesium-base solid solution materials with practical reliability via the solid-state synthesis. In the present project, this processing route is first applied to make solid state synthesis of ternary alloy compounds as the base of material optimum design toward high specific figure-of-merit and to demonstrate its capability of mass production to yield a massive amount of Mg2Si-base TE-leg materials.

Report Documentation Page

Form Approved
OMB No. 0704-0188

1. REPORT DATE	2. REPORT TYPE	3. DATES COVERED
08 FEB 2010	**FInal**	**03-08-2007 to 02-07-2009**

4. TITLE AND SUBTITLE
Improvement of thermoelectric-properties for Mg-based quaternary compounds with doping via bulk mechanical alloying

5a. CONTRACT NUMBER
FA48690814052

5b. GRANT NUMBER

5c. PROGRAM ELEMENT NUMBER

6. AUTHOR(S)
Tatsuhiko Aizawa

5d. PROJECT NUMBER

5e. TASK NUMBER

5f. WORK UNIT NUMBER

7. PERFORMING ORGANIZATION NAME(S) AND ADDRESS(ES)
Asia Science Education Economy Development,3-15-10 Minami-Rokugo, Ota-ku,Tokyo 144-0045,Japan,JP,1440045

8. PERFORMING ORGANIZATION REPORT NUMBER
N/A

9. SPONSORING/MONITORING AGENCY NAME(S) AND ADDRESS(ES)
AOARD, UNIT 45002, APO, AP, 96337-5002

10. SPONSOR/MONITOR'S ACRONYM(S)
AOARD

11. SPONSOR/MONITOR'S REPORT NUMBER(S)
AOARD-084052

12. DISTRIBUTION/AVAILABILITY STATEMENT
Approved for public release; distribution unlimited

13. SUPPLEMENTARY NOTES

14. ABSTRACT
In the magnesium base TE material design, the solid solution formation is favored for reduction of thermal conductivity by lattice scattering effect. Since magnesium and silicon have low relative density, Mg2Si-base TE compounds are expected to improve the specific figure-of-merit. In this project, new material processing route is proposed and developed to make material search for ternary or quartic TE compounds and to make mass-production of Mg2Si-base TE materials. Effect of Si, Ge and Sn on the thermoelectricity is also discussed to find an optimum way of TE-materials design.

15. SUBJECT TERMS
Energy Conservation, thermoelectric material, figure of merit

16. SECURITY CLASSIFICATION OF:			17. LIMITATION OF ABSTRACT	18. NUMBER OF PAGES	19a. NAME OF RESPONSIBLE PERSON
a. REPORT	b. ABSTRACT	c. THIS PAGE			
unclassified	**unclassified**	**unclassified**	**Same as Report (SAR)**	**20**	

Experiment:

Intense straining to drive the solid-state synthesis is applied to a starting material by the bulk mechanical alloying (BMA). As a starting material, the elemental powders are prepared with sufficiently high purity as shown in Fig. 1. In the following studies, elemental powders with the average size of 10 – 100 μm are used. The present experimental procedure is applicable even when starting from elemental granules or platelets in the order of millimeter. That is, this processing is free form size and morphology of initial matters. Our developed system is shown in Fig. 2. This system is composed of three parts; loading machine, sequence control unit and PC-based controller. Since loading is applied to the sample in the closed die cavity from upper and lower directions, the initial powder mixture is forced to be compressed, extruded elongated and re-combined in a cyclic manner. After homogeneous blending, each elemental powder mixture is subjected to bulk mechanical alloying in a flowing argon atmosphere to prevent the powder compact from oxidation. A core of this BMA is composed of die and special tools in Fig. 2. Different from the conventional mechanical alloying, no vials or balls are used. Since they are made form cemented carbide and hard tool steels, no contamination is expected to occur during BMA even when the initial elemental mixture is subjected to intense straining. The elemental powder mixture is pored into a die cavity to undergo the cyclic loading at room temperature. Since the die set is forced to cool down, temperature rise is kept low less than 40 K. In the present BMA system, the pass schedule with one forward extrusion and two compression modes is normally employed for above cyclic loading. To be noticed, every BMA sample is controlled to have relatively high density although BMA processes; in the following experiments, its relative density is kept constant, 80 % T.D. (true density).

Spark-plasma sintering as well as hot pressing, are available for densification of BMA samples and for net-shaping. In the following experiments, hot pressing system is used for high-pressure densification. The whole pressing die and tools are made from nickel-base superalloy in order that hot pressing operates up to 1273 K. In this hot pressing, pressure and holding temperature must be optimized to attain full density without significant grain growth. In the following experiments, the pressure is applied by 1 GPa at 773 K. Fully dense samples are successfully obtained by this condition.

X-ray diffraction (XRD) analysis with the monochromatic Cu K_α radiation is used to describe the soli d-state reaction via BMA. Scanning electron microscopy (SEM) with the energy dispersive X-ray sp ectroscopy (EDX) is utilized to observe the microstructure and to determine actual chemical compositi on of BMA samples. Transmission electron microscopy (TEM) is also used to detect the embryo of s ynthesized compound during BMA.

The differential thermal analysis (DTA) is carried out to explore the onset-temperature of solid-state re action during BMA process with the heating rate of 20 K/min up to 1073 K in an argon atmosphere w hen using Shimadzu DTG-60.

The samples for thermoelectric measurement are cut out from hot-pressed pellets. A rectangular bar with the size of 2 x 2 x 8 mm^3 is fabricated for measurement of the Seebeck coefficient and the electrical conductivity. A circular disc with the diameter of 10 mm and the thickness of 2 mm is used for measurement of thermal conductivity. The thermoelectric properties are evaluated from the room temperature up to 700 K. The Seebeck coefficient (α) and the electrical conductivity (σ) are simultaneously measured by the four-probe dc method in helium atmosphere, using the computer-controlled equipment. The thermal conductivity (κ) and the specific heat capacity (C_p) are measured by the laser flash methods, using a thermal constant analyzer (ULVAC TC-7000) in vacuum. The thermal conductivity is calculated from the measured thermal diffusivity, specific heat capacity and bulk density (d): $k = DC_pd$. The bulk density of the hot-pressed samples is measured by the Archimedes method.

Results and Discussion: Describe the results obtained during the period of performance and what work may be performed in the future as follow on.

[1] Demonstration of solid-state synthesis of single-phase, Mg_2Si via solid-state synthesis

Bulk mechanical alloying was used to make solid-state synthesis of Mg_2Si from the blended p owder mixture of Si and Mg. XRD and DTA were used to describe this synthesis process. XRD profile was measured at the specified number of cycles (N) in BMA in order to investigate the solid-state reaction during BMA. Figure 3 depicts the change of XRD profiles for the BMA samples with increasing the number of cycles. When N = 0 or in as-blended samples, triplet peaks for magnesium and characteristic peaks to silicon are detected. These peak intensities reduce with increasing N. In the case of Mg-Si system, gradual reduction of peak intensities is observed for N < 500 and is followed by abrupt change of XRD profile between N = 500 and N = 600. The single phase of Mg_2Si is obtained when N = 600. This solid-state reaction behavior is also described by DTA. Since the formation enthalpy for Mg_2Si is positive, the typical exothermic peaks are detected near the endothermic peak for melting of magnesium when N = 0 in Fig. 4. This exothermic peak intensity reduces gradually with N while the peak temperature shifts itself to the lower temperature side. When N = 600, no peaks are detected both in heating and cooling processes in DTA. This assures that the whole of magnesium is reacted with silicon to form a single phase of Mg_2Si. From the exothermic peak in DTA diagram, the formation enthalpy of reaction (ΔH_f) is estimated for each BMA sample. When t = 0, the measured formation enthalpy of Mg_2Si from DTA diagram is ΔH_f^0 = 68 kJ/mol while ΔH_f = 77.3 kJ/mol in literature This difference comes from the fact that the exothermic peak intensity measured from DTA diagram is underestimated by overlapping of endothermic peak on it.

Mg_2Si is extraordinarily high among Mg_2X like $|\alpha|$ = -700 to -800 μVK^{-1}. Due to intrinsic semi-conductivity, Mg_2Si has much lower electrical conductivity around the room temperature. Mg_2Sn has much higher electrical conductivity. The bandgap for Mg_2Si becomes Eg = 0.71 eV. This value is in good agreement with the reported data in literature. This assures that this type of binary semi-conductive and metallic compounds, Mg_2Si, should be yielded with accurate chemical composition. The effect of refinement via BMA on the thermoelectricity is observed in the thermal conductivity data. The thermal conductivity (κ_{RT}) at room temperature for a single-crystalline Mg_2Si is 7.8 $Wm^{-1}K^{-1}$; κ_{RT} is 4.8 $Wm^{-1}K^{-1}$ or less than for BMA samples. This low thermal conductivity is much favored for this Mg base thermoelectric material design.

[2] Solid solution formation of Mg-Si-Ge compound via solid-state synthesis

The initial elemental powder mixture is blended with the specified molar ratio and prepared for BMA; in this experiment, the initial molar ratio is selected to be equivalent to $Mg_2Si_{0.6}Ge_{0.4}$. In order to investigate the solid-state reaction during BMA, variation of XRD profiles was measured at the specified number of cycles (N) in BMA. Figure 5 depicts the change of XRD patterns for BMA samples with Mg 66.6 at%, Si 20.0 at% and Ge 13.4 at% at N=0, 100, 200, 300, 400, 500 and 600. Peaks for Mg (hcp-structured with a = 0.3209 nm and c = 0.5211 nm), Si (diamond-structured with a = 0.5431 nm) and Ge (diamond-structured with a = 0.5658 nm) are detected in the blended sample at N = 0. Peak intensities of these elements reduce with increasing the number of cycles for N < 300. The peaks for cubic-structured $Mg_2Si_{0.6}Ge_{0.4}$ solid solution phase are detected for N > 300. When N=500, most of peaks for Mg, Si and Ge diminish in the trace level; the single phase of $Mg_2Si_{0.6}Ge_{0.4}$ is synthesized when N=600.

DTA is also employed to describe the solid-state reaction behavior. Figure 6 depicts the variation of DTA profiles with N. When N = 0, or, for the as-blended powder mixture, an exothermic peak as well as two endothermic peaks are distinctly detected. This exothermic peak corresponds to the formation of Mg_2Si and Mg_2Ge from the elemental powder mixture. Two endothermic peaks respectively correspond to the melting of magnesium and germanium. Detection of the first endothermic peaks for N < 300, reveals that unreacted magnesium is still left in the sample. The onset temperature to ignite the reaction to Mg_2Si and Mg_2Ge is shifted to the lower temperature side with increasing the number of cycles. When N = 500, no exothermic nor endothermic peaks are seen in DTA. No difference is recognized in DTA diagram between two samples at N = 500 and N = 600. This also assures that the initial, elemental powder mixture is fully reacted in solid to $Mg_2Si_{0.6}Ge_{0.4}$. The BME sample at N = 600 has compositions of Mg 66.4 at%, Si 20.4 at% and Ge 13.2 at% after EDX analysis. This assures that the solid state synthesis from elemental powder mixture yields any solid solution type compounds with accurate chemical composition.

Variation of the Seebeck coefficient (α) with temperature is depicted in Fig. 7 for $Mg_2Si_{1-x}Ge_x$ samples, hot-pressed at 773K by 1GPa. Its absolute value ($|\alpha|$) decreases with temperature irrespective of the germanium content (x) since the number of carriers increases by thermal activation. The highest Seebeck coefficient is attained at room temperature for Mg_2Si and $Mg_2Si_{0.6}Ge_{0.4}$: e.g., $|\alpha|$ = 800 μV/K. Here to be interested is a p-n transition between x = 0.2 and x = 0.4. When x = 0.2, α is negative, and, both $Mg_2Si_{0.8}Ge_{0.2}$ as well as Mg_2Si are n-type. α turns to be positive for x > 0.4 and $Mg_2Si_{1-x}Ge_x$ becomes p-type.

[3] Optimum alloy design for Mg_2Si-based TE-leg materials

Mg_2Si-base system like Mg-Si-Ge-Sn is attractive since its TE-properties are controllable by tuning the contents of silicon, germanium and tin even without doping. As shown in Fig. 7, both p- and n-leg materials are prepared in Mg-Si-Ge solid solution owing to the p-n transition; i.e. Mg2Si1-xGex plays as an n-type leg for x < 0.3 and as a p-type leg for x > 0.4. This system has high Seebeck coefficient but low electrical conductivity. Then, the forth element had better be added to this system like tin. Figure 8 depicts the increase of electrical conductivity with increasing the holding temperature for Mg2Si1-ySny and 0 < y < 1. Improvement of electrical conductivity for $Mg_2Si_{1-x-y}Ge_xSn_y$ is attained by small addition of Mg_2Sn with y < 0.1. In fact, p-type $Mg_2Si_{1-x-y}Ge_xSn_y$ with x = 0.5 and y = 0.1 is synthesized to have S = 500 μVK^{-1}, s = 4 x 10^4 $W^{-1}m^{-1}$ and κ = 3 $Wm^{-1}K^{-1}$ at 400 K. This provides higher figure-of-merit: Z = 3.4 x 10^{-3} K^{-1} and ZT = 1.3. Further improvement of Z and ZT could be attained with optimum doping to this system.

[4] New processing route to mass-production of TE-leg materials

In the mass production of TE-leg materials, energy efficiency in fabrication must be also improved as possible to reduce the turn-back time for TE-modules. In the present solid-state synthesis, reduction of loading cycles directly results in reduction of energy. Figure 9 shows the variation of XRD and DTA profiles with N for N < 200. No peaks of synthesized Mg_2Si were seen in XRD profile at N = 150 while significant reduction of ignition temperature for solid state reaction to Mg2Si is noticed. Fig, 10 compares the microstructure of initial powder mixture at N = 0 and BMAed sample at N = 150. Fine mixture state of magnesium and silicon might play a role to enhance the solid-state reaction to Mg2Si as shown in Fig. 9. This suggests that Mg_2Si could be directly synthesized by low-temperature heat treatment of BMAed sample.

Fig, 11 compares the variation of XRD profiles at different temperatures in heat treatment between initial powder mixture and BMAed sample by N = 150. Heat treatment at T = 623 K is enough to ignite full reaction to Mg_2Si from BMAed sample by N = 150. This measurement is demonstrated by microstructure observation in Fig. 12. In case of initial powder mixture, silicon residuals are still left in the system even after heat treatment for 1 hr at T = 1003 K above the melting point of magnesium. Full reaction was attained in the heat treatment of BMAed sample at T = 623 K. Thermo-electric properties of this heat-treated sample were measured. Figure 13 shows the variation of electrical conductivity with increasing the holding temperature. Measured bandgap was found to be in fairly good agreement with the reference data in the literature. This proves that this sample should be intrinsic semi-conductive Mg_2Si. That is, the above process is responsible for mass production of Mg_2Si-based TE-leg materials.

The above enhancement of solid-state reactivity is attributed to nucleation of Mg2Si-embryo during the bulk mechanical alloying. Figure 14 shows a typical TEM micrograph of BMAed sample at N = 150. Mg2Si-embryo is synthesized at the interface between magnesium and silicon phases in the BMAed sample. Solid-state reactivity is thought to be in close relationship with this formation of Mg2Si-embryo. Mock-up experiment was performed to discuss the possibility of mass production by using the above process. Figure 15 proves that BMEed sample with the weight of 300 to 500g is directly yielded by bulk mechanical alloying.

References

1) R.J. Laboz, D.R. Mason and D.F. Okane: J. Electrochemistry. Soc. 110 (1963) 127-134.
2) Y. Noda: *Thermoelectric Technology*. Fuji-Techno-System. (2000) 217-229.
3) M.I. Fedrov and V.K. Zaitsev: Prof. 19th Int. Conf. on Thermoelectrics (Cardiff, UK, 2000) 17-27.

4) Y. Noda, N. Otsuka, K. Masumoto and I.A. Nishida: J. Appl. Phys. 53 (1989) 487-491.
5) Y. Noda, H. Kon, Y. Fushitaka, N. Otsuka, I. Nishida and K. Masumoto: Mater. Trans. JIM 53 (1992) 844-850.
6) Y. Noda, H. Kon, Y. Fushitaka, N. Otsuka, I. Nishida and K. Masumoto: Mater. Trans. JIM 53 (1992) 851-855.
7) T. Schilz, M. Riffel, K. Pixius and H.-J Meyer: Powder Metallurgy. 105 (1999) 149-154.
8) C.R. Clark, C, Wright, C. Suryanarayana, E.G. Baburaj and F.H. Froes: Mater. Letter. 33 (1997)

List of Publications: Please list any publications, conference presentations, or patents that resulted from this work.

T. Aizawa: Solid-State Synthesis of Magnesium-Based Functional Alloys and Compounds. Trans Tech Publications (2009). ISSN 1422-3597.

DD882: As a separate document, please complete and sign the inventions disclosure form.

This document may be as long or as short as needed to give a fair account of the work performed during the period of performance. There will be variations depending on the scope of the work. As such, there are no length or formatting constraints for the final report. Include as many charts and figures as required to explain the work. A final report submission very similar to a full length journal article will be sufficient in most cases.

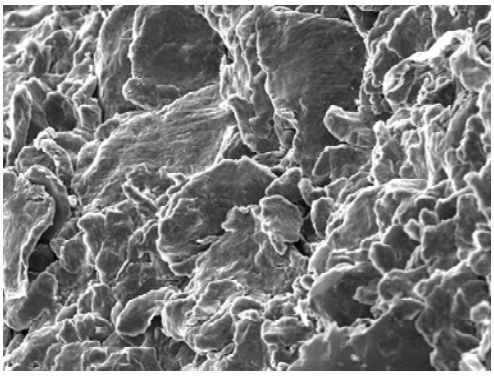

Mg

Mg (99.9%, 100μ m)

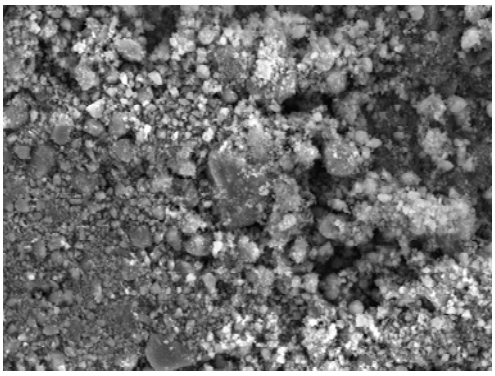

Si

Si (99.99%, 20μ m)

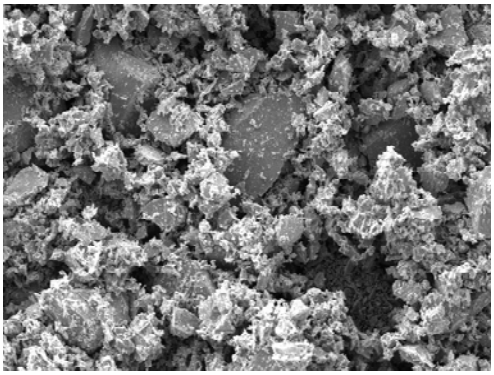

Ge

Ge (99.999%, 100μ m)

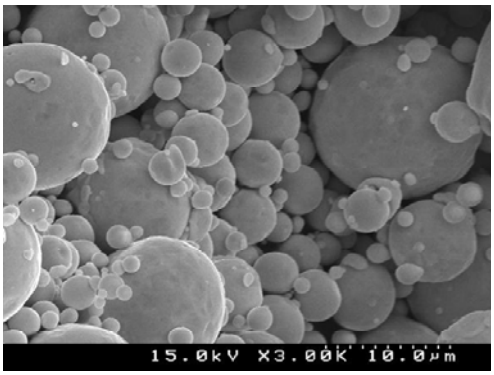

Sn

Sn (99.9%, 10μ m)

Fig. 1: Starting element powders: Mg, Si, Ge and Sn.

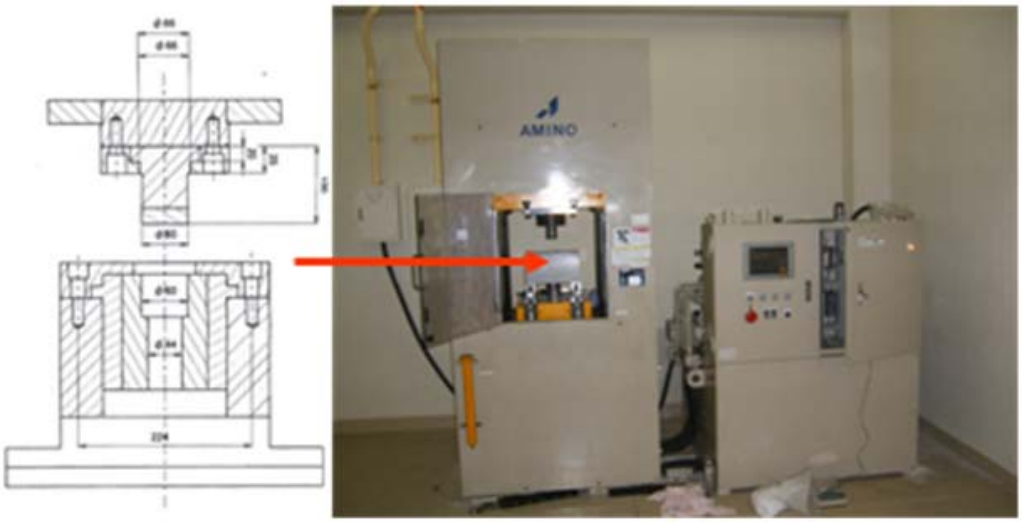

Fig. 2: Newly developed bulk mechanical alloying system and die-set for mass-production of Mg_2Si-based TE compounds.

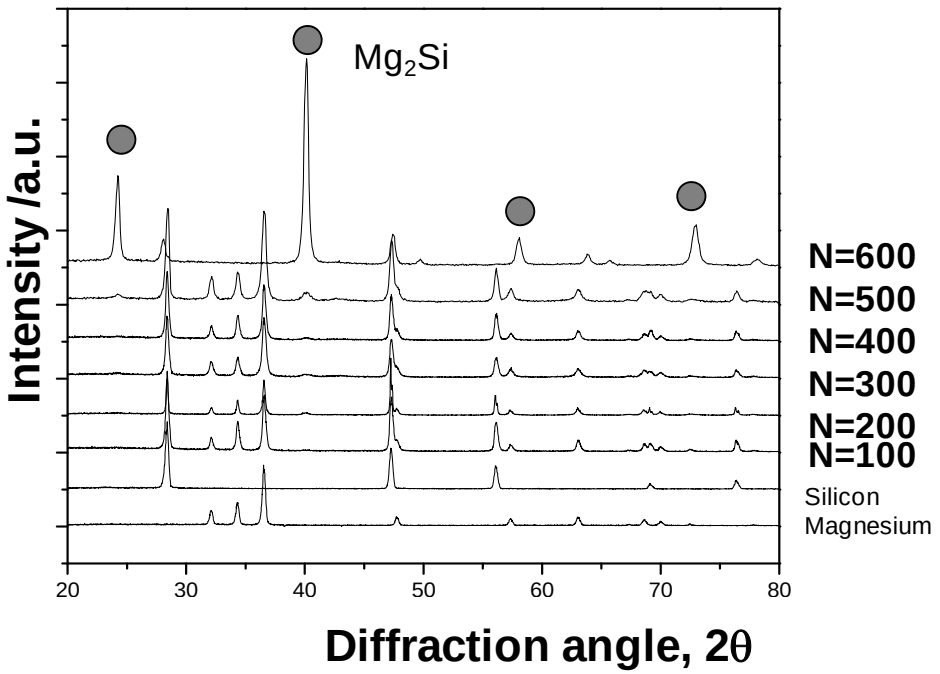

Fig. 3: Variation of XRD profiles with increasing the number of loading cycles (N) in the solid-state synthesis via the developed bulk mechanical alloying system.

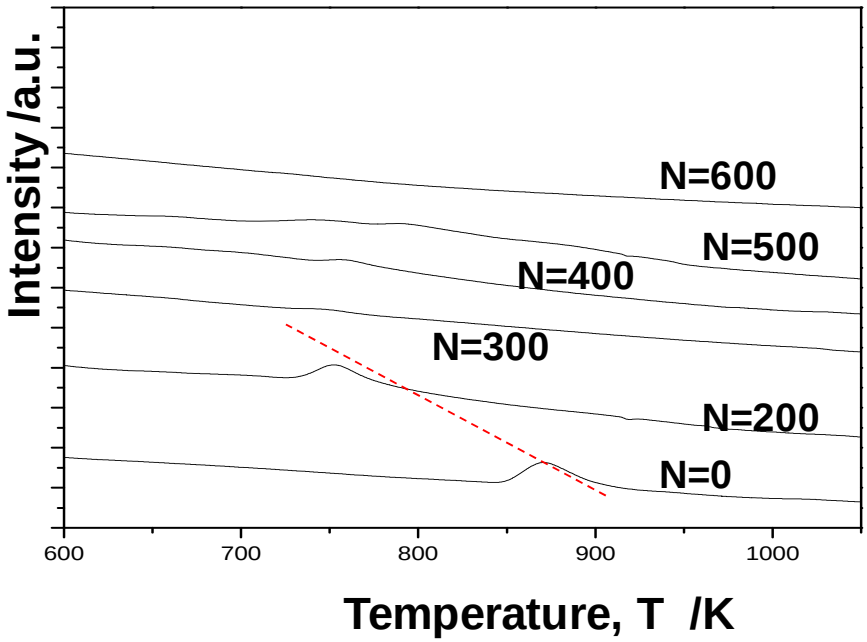

Fig. 4: Variation of DTA profiles with increasing the number of loading cycles (N) in the solid-state synthesis via the developed bulk mechanical alloying system.

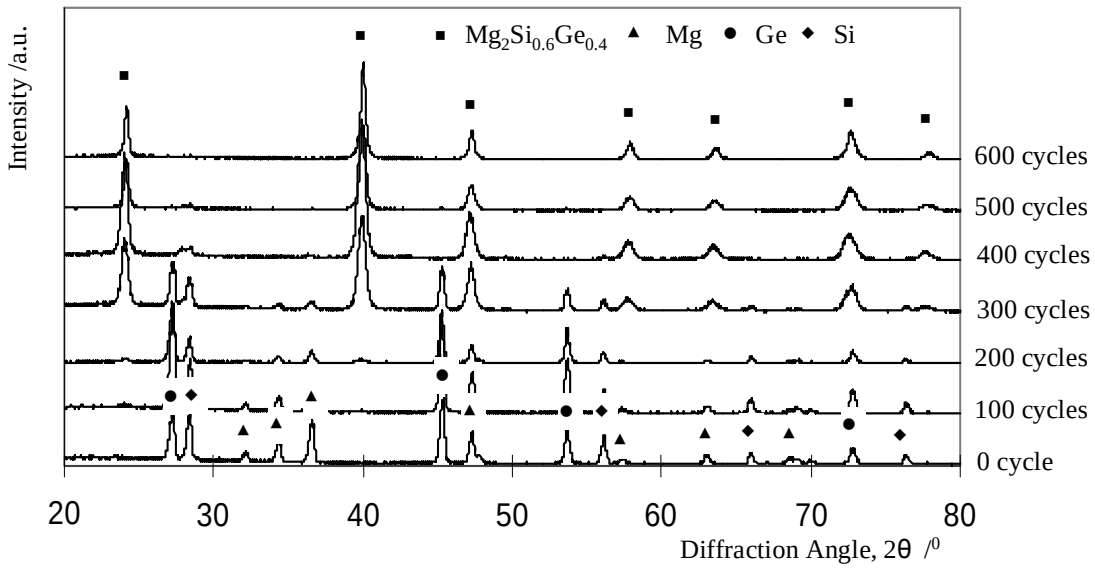

Fig. 5: Variation of XRD profiles with increasing the number of loading cycles (N) starting from the elemental powder mixture of Mg, Si and Ge with the initial molar ratio of $Mg_2Si_{0.6}Ge_{0.4}$.

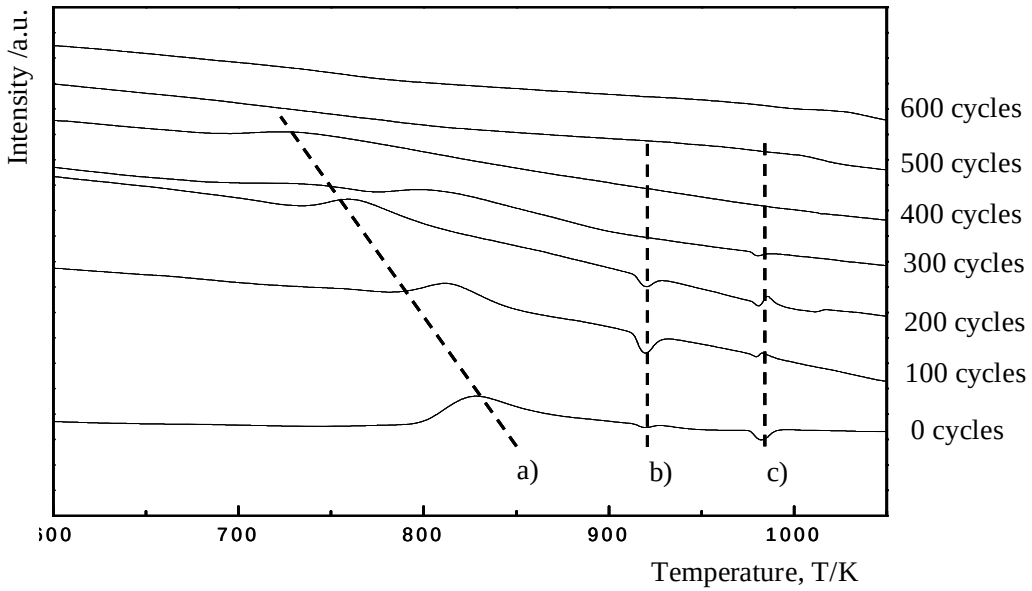

Fig. 6: Variation of DTA profiles with increasing the number of loading cycles (N) starting from the elemental powder mixture of Mg, Si and Ge with the initial molar ratio of $Mg_2Si_{0.6}Ge_{0.4}$.

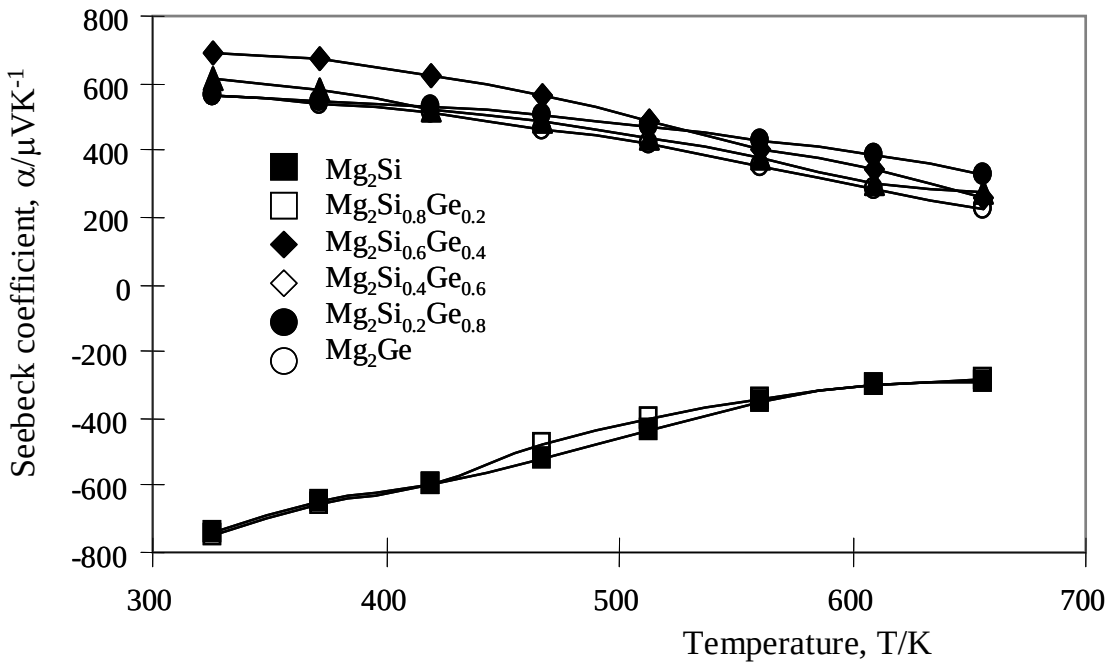

Fig. 7: Variation of Seebeck coefficient with increasing the holding temperature for $Mg_2Si_{1-x}Ge_x$ and $0 < x < 1$.

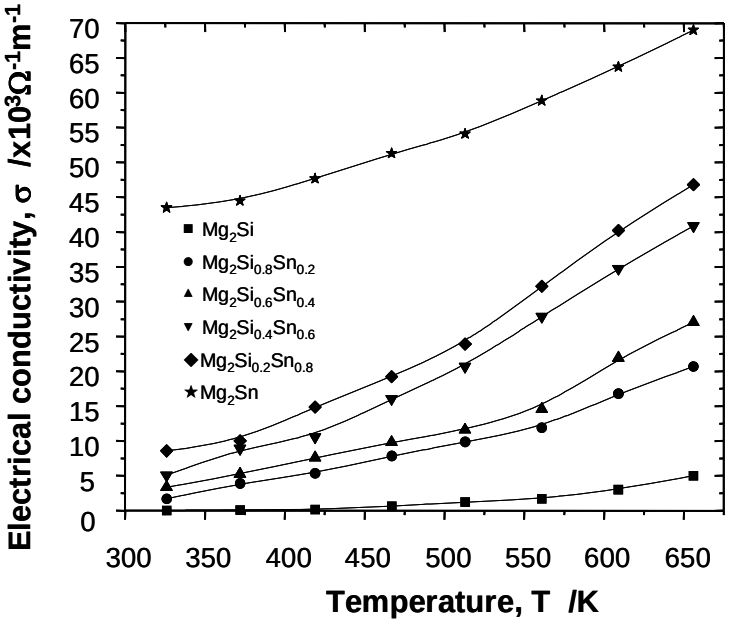

Fig. 8: Variation of electrical conductivity with increasing the holding temperature for $Mg_2Si_{1-y}Sn_y$ and $0 < y < 1$.

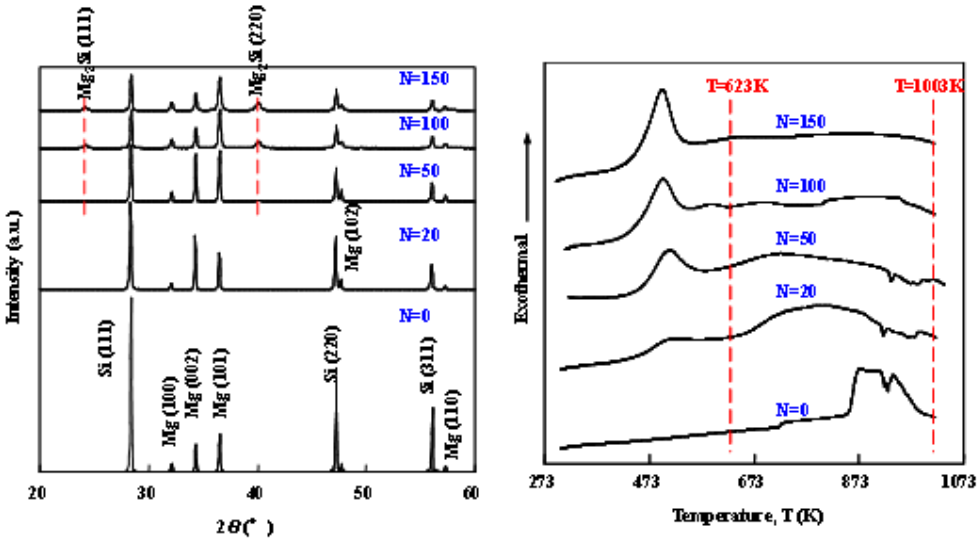

Fig. 9: Variation of XRD and DTA profiles with increasing the number of cyclic loading in the present bulk mechanical alloying.

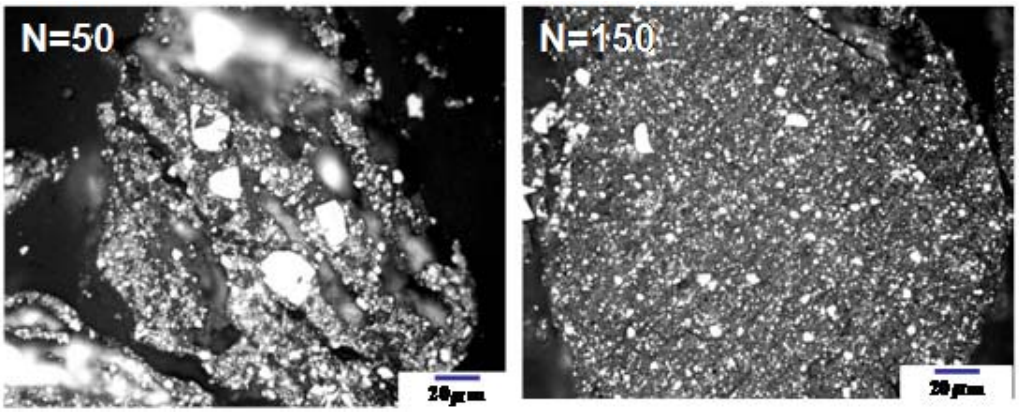

Fig. 10: Comparison of microstructure between BMAed samples at N = 50 and N = 150.

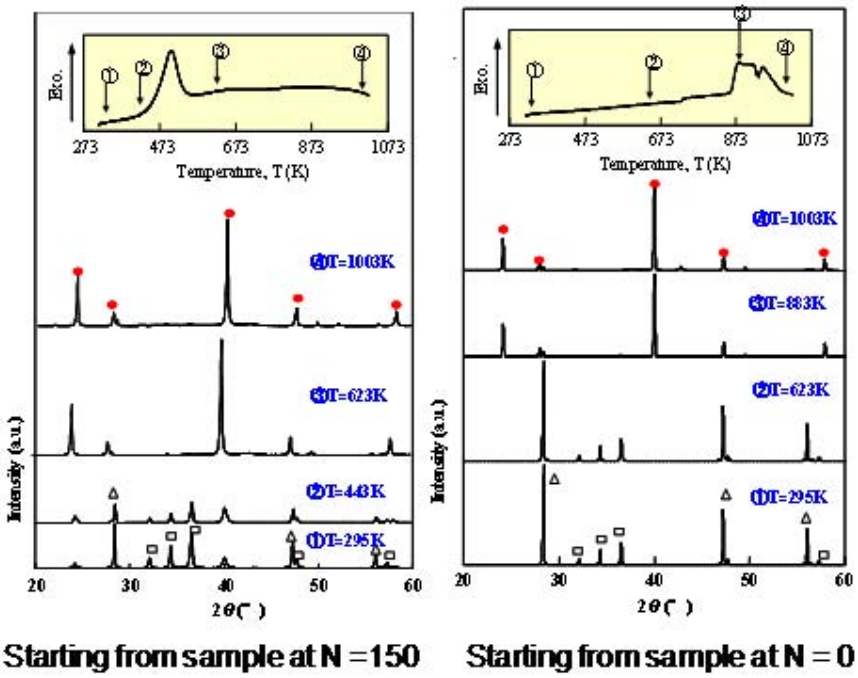

Fig. 11: Comparison of XRD profiles after heat treatment at the specified temperature (T) between the initial powder mixture at N = 0 and BMAed sample at N = 150.

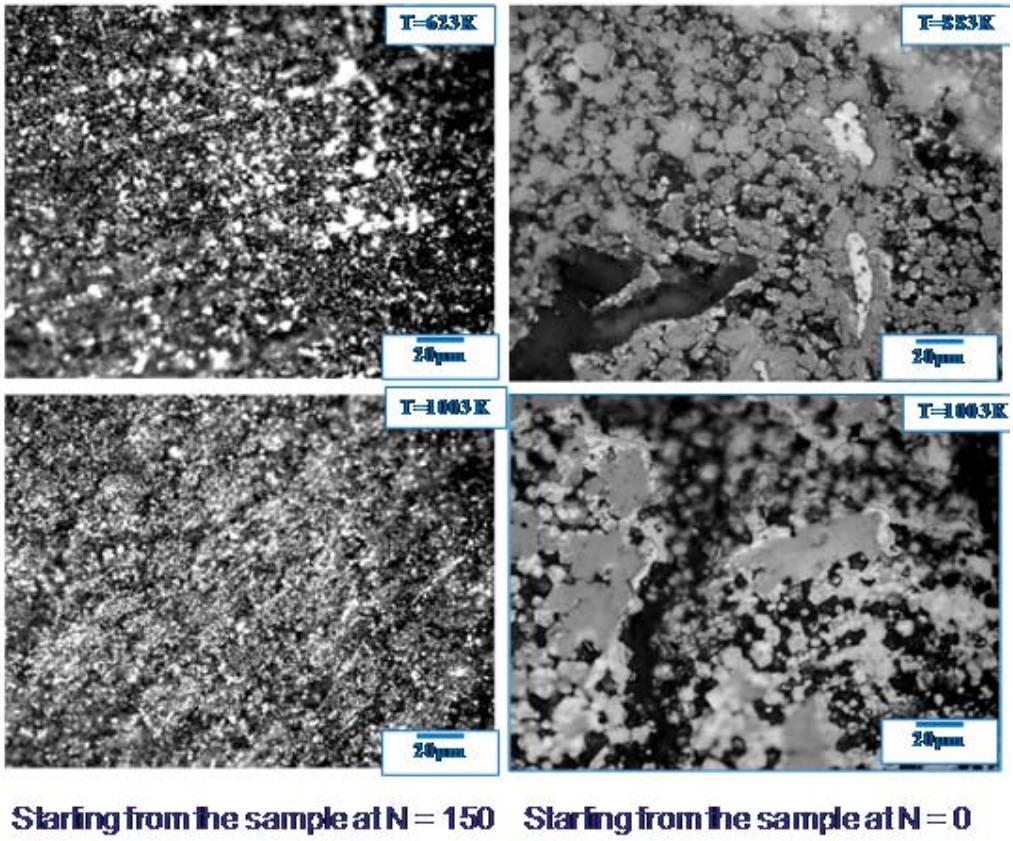

Fig. 12: Comparison of microstructure after heat treatment at the specified temperature (T) between the initial powder mixture at N = 0 and BMAed sample at N = 150.

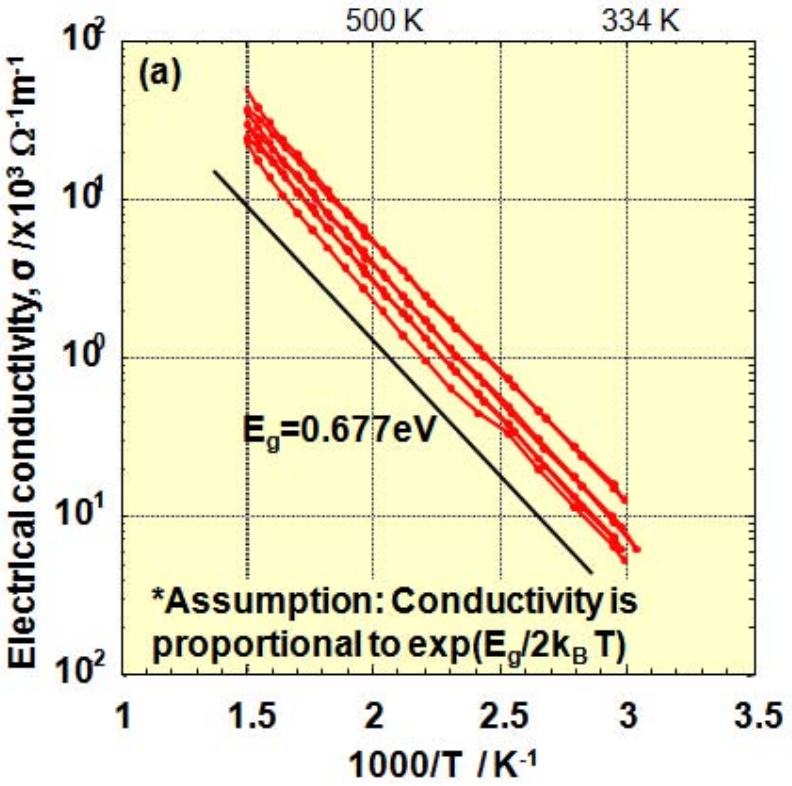

Fig. 13: Relationship of electrical conductivity to reciprocal temperature for BMAed sample after heat treatment.

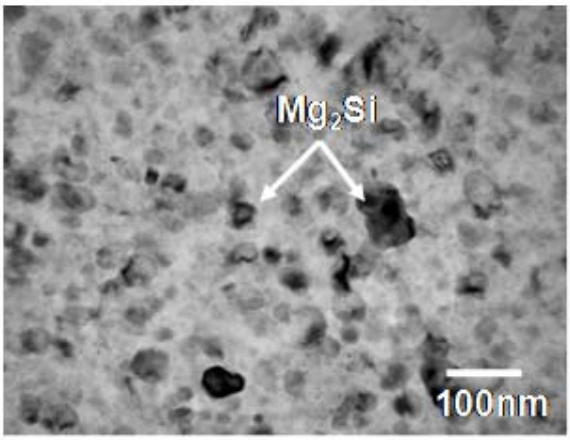

Fig. 14: TEM micrograph of Mg2Si embryo in the BMAed sample at N = 150.

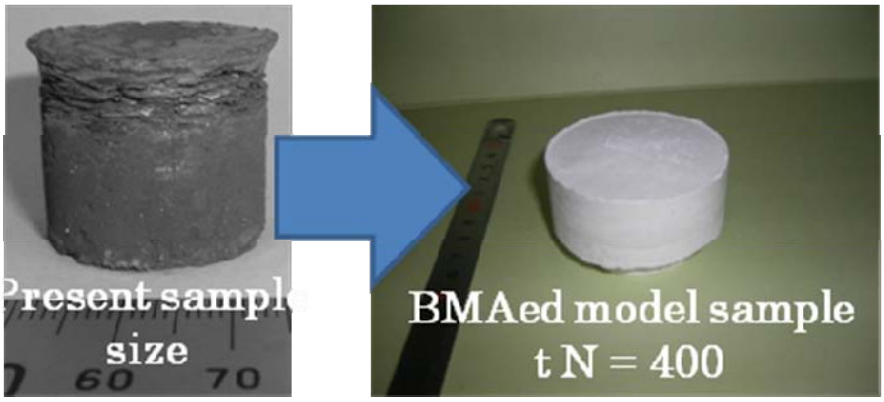

Fig. 15: Demonstration of scaling-up for BMA-originating materials process for mass-production of TE-leg materials.